

Cite this article as: Wang Jie, Zhang Yiwei, Xiong Yanlin, et al. Effects of Bonding Time on Microstructure and Mechanical Properties of  $Ti_3Al/Ti_2AlNb$  Joint Prepared by Transient Liquid Phase Diffusion Bonding[J]. Rare Metal Materials and Engineering, 2022, 51(12): 4446-4451.

ARTICLE

# Effects of Bonding Time on Microstructure and Mechanical Properties of $Ti_3Al/Ti_2AlNb$ Joint Prepared by Transient Liquid Phase Diffusion Bonding

Wang Jie<sup>1</sup>, Zhang Yiwei<sup>1</sup>, Xiong Yanlin<sup>1</sup>, Yang Jin<sup>2</sup>, Feng Yang<sup>1</sup>

<sup>1</sup>School of New Energy and Materials, Southwest Petroleum University, Chengdu 610000, China; <sup>2</sup>Chengdu Sky Combustion Control Technology Co., Ltd, Chengdu 610500, China

**Abstract:** Using Ni-Ti duplex foils as joining materials,  $Ti_3Al$  alloy was bonded to  $Ti_2AlNb$  alloy by transient liquid phase (TLP) diffusion bonding at 990 °C under low bonding pressure (0.1 MPa). The effects of bonding time on the microstructure and mechanical properties of  $Ti_3Al/Ti_2AlNb$  joint were analyzed, as well as the interfacial evolution and forming mechanism of the TLP joint were studied. Results show that the  $Ti_3Al/Ti_2AlNb$  alloy joints with typical interface structure of  $Ti_3Al | Al_{0.5}Nb_{0.5}Ti_3 | residual Ni | NiTi | NiTi_2 | residual Ti | Al_{0.5}Nb_{0.5}Ti_3 | Ti_2AlNb$  can be formed. In addition, with the extension of bonding time, the shear strength of the joint first increases and then decreases, and the maximum shear strength, up to  $167 \pm 12$  MPa, of the  $Ti_3Al/Ti_2AlNb$  alloy joint can be achieved when the bonding time reaches 60 min. The joint fracture, characterized by brittle fracture, mainly occurs at the  $NiTi_2$  layer adjacent to the  $Ti_2AlNb/Ti$  interlayer and extends to the Ti interlayer.

**Key words:**  $Ti_3Al$ ;  $Ti_2AlNb$ ; transient liquid phase (TLP); diffusion bonding; interface structure

As high-temperature structural materials with great development potential,  $Ti_3Al$  and  $Ti_2AlNb$  alloys have excellent properties such as high elastic modulus, high specific strength, excellent creep resistance and high-temperature oxidation stability. Though both of them have broad application prospects in aerospace and other fields,  $Ti_3Al$  alloy has relatively lower density, insufficient toughness and plasticity compared with  $Ti_2AlNb$  alloy<sup>[1-5]</sup>. If we can give full play to their respective performance advantages and make  $Ti_3Al$  and  $Ti_2AlNb$  alloy into composite components with excellent comprehensive performance, more choices and references for the design and manufacture of related components may be provided in the future. Therefore, it is of great significance to study the joining of  $Ti_3Al$  and  $Ti_2AlNb$  alloy for the preparation of advanced composite components and the expansion of their application fields<sup>[6-10]</sup>.

At present, fusion welding<sup>[11,12]</sup>, brazing<sup>[13]</sup> and diffusion bonding<sup>[14]</sup> are the commonest three joining techniques, and they all have their own advantages and disadvantages. With

the continual generating of new materials, brazing and diffusion bonding have been widely used in materials processing field. In particular, transient liquid phase (TLP) diffusion bonding has attracted more and more attention in the joining of special materials, new materials and dissimilar materials since it combines the advantages of brazing and diffusion bonding<sup>[15-18]</sup>. Some scholars have successfully bonded the  $Ti_2AlNb$  alloy to other alloy materials by TLP diffusion bonding using nano-laminated Cu-Ti foil as interlayer. The experiment results show that the joint has the maximum room temperature shear strength of 305 MPa under the high bonding pressure of 20 MPa. Moreover, for large and complicated components, it will be limited by the inconvenience of exerting big bonding pressure. At present, there are few reports on the bonding of  $Ti_3Al$  alloy to  $Ti_2AlNb$  alloy by TLP diffusion bonding, especially under low bonding pressures. It should be noted that the type of interlayer is a key factor for the properties of the joint. In Ref. [19], the mechanical properties of TiAl joints with Ni-Ti as interlayer

Received date: February 18, 2022

Foundation item: National Nature Science Foundation of China (51602269)

Corresponding author: Wang Jie, Ph. D., Associate Professor, School of New Energy and Materials, Southwest Petroleum University, Chengdu 610000, P. R. China, Tel: 0086-28-83037416, E-mail: wangjie@swpu.edu.cn

Copyright © 2022, Northwest Institute for Nonferrous Metal Research. Published by Science Press. All rights reserved.

are better than those with Ti-Cu-Ni as interlayer.

Therefore, in the present study, the TLP diffusion bonding experiments of  $Ti_3Al$  and  $Ti_2AlNb$  alloy were conducted using Ni-Ti duplex foils as interlayer under low bonding pressure, and the microstructure, mechanical properties and formation mechanism of as-prepared  $Ti_3Al/Ti_2AlNb$  joints were also studied.

## 1 Experiment

In this experiment, the parent alloys were  $Ti_3Al$  (Ti-23Al-17Nb, at%) and  $Ti_2AlNb$  (Ti-17Al-25Nb, at%) alloy, provided by Central Iron and Steel Research Institute. The former mainly consists of  $\alpha_2$  phase,  $B_2$  phase and primary lamellar O phase and the latter generally consists of two or three phases of  $\alpha_2$ ,  $\beta/B_2$  and primary lamellar O phase. Both  $Ti_3Al$  alloy and  $Ti_2AlNb$  alloy were processed into 10 mm×10 mm×5 mm rectangle specimens by the wire cutting machine. The surfaces of parent materials for joining were polished step by step with 240#~600# SiC sandpaper, and the surface of interlayer foil, i.e. Ni foil and Ti foil with 30  $\mu m$  in thickness, was polished with 1000# SiC sandpaper. The samples and interlayers were ultrasonically cleaned in alcohol and dried at 85 °C for 1.5 h. After that, the Ni foil and Ti foil were set between  $Ti_3Al$  alloy and  $Ti_2AlNb$  alloy to constitute a sandwich structure ( $Ti_3Al|Ni-Ti|Ti_2AlNb$ , Fig. 1a). During the joining procedure, a low pressure (~0.1 MPa) was used for compressing specimens. This assembly was heated up to 800 °C at the rate of 10 °C/min firstly, and then bonding temperature was continuously increased to 990 °C at 5 °C/min and kept stable for 10~90 min by the vacuum diffusion-bonding machine under the vacuum atmosphere of  $3\times 10^{-2}$  Pa. After the prepared joints were cooled to about 25 °C, they could be taken out from the vacuum diffusion-bonding machine. The joints were successively ground by 240#~5000# SiC sandpaper gradually, etched with the solution of 2 mL HF-5 mL  $H_2O_2$ -100 mL  $H_2O$ , polished with polishing agent, washed in alcohol by ultrasonic cleaning, and finally dried by electric hair dryer for microscopic observation and analysis. The microstructure and fracture morphology of joint were investigated by ZEISS EV0 MA15 scanning electron microscope (SEM), and the element distribution of cross section of joint and fracture surface was tested by energy-dispersive spectroscopy (EDS). The phases on fracture surfaces were characterized by DX-2700 X-ray

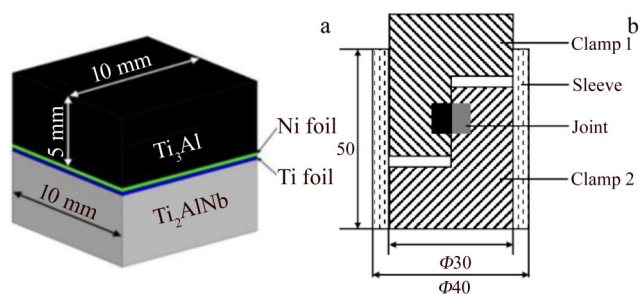


Fig.1 Diagram of the joint assembly (a) and device for shear testing (b)

diffraction (XRD) with Cu-K $\alpha$  radiation. As displayed in Fig.1b, the shear strength test was conducted on a WDW-1000 universal testing machine with a stable speed of 0.5 mm/min by a set of clamps. The joint shear strength value ( $W$ ) was computed by the follow equation:

$$W=P/F \quad (1)$$

where  $W$  is the joint shear strength (MPa),  $P$  is the maximum load (N) and  $F$  is the bonding area ( $mm^2$ ). The final shear strength of the joint was obtained by calculating the average of four effective shear strengths in the experiment.

## 2 Results and Discussion

### 2.1 Typical microstructure of $Ti_3Al/Ti_2AlNb$ joints

Fig. 2 displays the typical interfacial microstructure and corresponding EDS line-scan result of the  $Ti_3Al/Ni/Ti_2AlNb$  joint obtained at 990 °C for 30 min. It is obvious that the sound joint with an interlayer (~73  $\mu m$ ) is obtained, where defects such as cracks and pores are almost non-existent. According to Fig.2a and 2b, the interlayer mainly consists of four different zones (named as I, II, III, IV), in which layer I (~10  $\mu m$ ) and layer IV (~33  $\mu m$ ) are the transition zones adjacent to the parent materials, layer II (~17  $\mu m$ ) and layer III (~13  $\mu m$ ) are the residual interlayers. To explore the element diffusion in the joining process, the distribution of dominating elements across the joint (along the white base line) was conducted by the line-scan analysis (Fig. 2b). The content of Al and Nb in the whole interlayer is very low, which indicates that very little Al and Nb of the base material are dissolved and difficult to diffuse into the interlayer. In order to further analyze the components in the joint, element distribution of the joint cross section was analyzed by EDS,

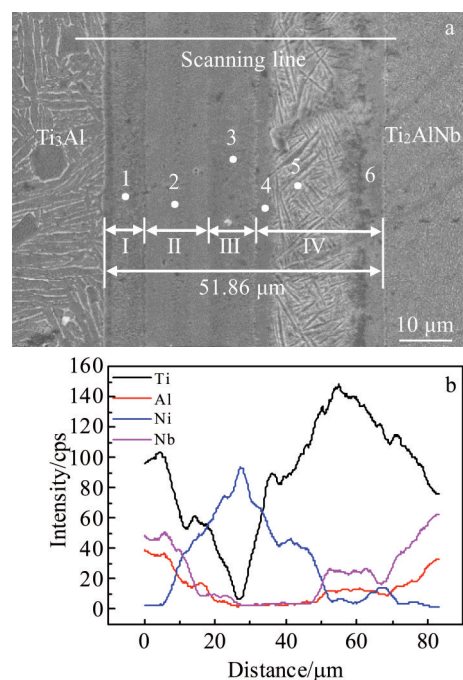


Fig.2 Microstructure (a) and EDS line-scanning results (b) of  $Ti_3Al/Ti_2AlNb$  joint obtained at 990 °C for 30 min

and the XRD analysis of the fracture surface of joints after shear test was conducted. Combining the EDS results (Table 1) and XRD analysis results (Fig.3b), white flaky and acicular materials located in point 1 and 5 are  $Al_{0.5}Nb_{0.5}Ti_3$ , while point 2 and 5 are residual Ni and Ti layers; based on the atomic percentage, point 3 and 4 are probably NiTi and  $NiTi_2$ , respectively. Therefore, the stratified structure of the joint is as follows:  $Ti_3Al | Al_{0.5}Nb_{0.5}Ti_3 | residual Ni | NiTi | NiTi_2 | residual Ti | Al_{0.5}Nb_{0.5}Ti_3 | Ti_2AlNb$ .

## 2.2 Effects of bonding time on microstructure of $Ti_3Al/Ti_2AlNb$ joints

Fig.4 displays the interface structure and EDS line scanning results of the joint obtained at 990 °C for 10, 60 and 90 min. It can be observed that the bonding time has a striking impact on the interface microstructure of the joints. When bonding time is 10 min, there are obvious cracks, holes and stratification at the joining interface due to the short bonding time, and the joint elements can only react locally with low diffusion efficiency, especially the Ni element, which generates less reactants at the interface. From Fig.2 and Fig.4, the overall widths of the interlayer treated for 10, 30, 60 and 90 min are 37.69, 51.86, 61.14 and 21.59  $\mu m$ , respectively. With the extension of bonding time, the more the element diffusion, the better the chemical reaction. The overall width of the interlayer increases first and then decreases, and the thickness of residual interlayer becomes thinner, while the thickness of transition layer of adjacent parent materials increases. When bonding time reaches 90 min,  $Ti_3Al$  base materials undergo phase transition due to longer time. With the continuous atomic diffusion, the more the  $\alpha_2$  phase is dissolved, the more the corresponding  $B_2$  phase becomes available, which eventually decreases the content of  $\alpha_2$  phase and coarsens the grain of  $B_2$  phase. Meanwhile, the white acicular material adjacent to  $Ti_2AlNb$  is diminished or even disappears with the formation of new black flaky material. With the increase in temperature, black band-like and black block-like areas form on both sides near  $Ti_3Al$  and  $Ti_2AlNb$ , respectively. Combined with the results of EDS line scanning, the substances of the two areas are very close, so it can be speculated that the nearby black flaky material is the  $B_2$ -rich phase.

## 2.3 Mechanical properties and shear fracture behavior of $Ti_3Al/Ti_2AlNb$ joints

Fig.5 displays shear strength of  $Ti_3Al/Ti_2AlNb$  joints versus bonding time. It is clear that the bonding time has a noticeable

effect on the mechanical properties of the  $Ti_3Al/Ti_2AlNb$  joint. The shear strength of joints treated for 10, 30 and 60 min achieves  $142\pm 5$ ,  $152\pm 9$ , and  $167\pm 12$  MPa, respectively. When the bonding time increases to 90 min, the joint shear strength expresses a slight decline with the value of  $160\pm 7$  MPa. On the one hand, too short bonding time will restrict the diffusion of elements, which results in incomplete reaction in the joint and is harmful to the strength of joint. On the other hand, when the bonding time increases to 90 min, the overlong bonding time will cause the  $Ti_3Al$  base material to undergo phase transition. Eventually the content of  $\alpha_2$  phase is decreased and the grain of  $B_2$  phase is coarsened. Meanwhile, the white acicular structure adjacent to  $Ti_2AlNb$  is diminished or even disappears with the formation of new black flaky material. Those are also an explanation why the joint treated for overlong bonding time has lower strength. Therefore, it is no doubt that selecting a proper bonding time is the key to prepare  $Ti_3Al/Ti_2AlNb$  joints with outstanding mechanical properties. In this study, the joint obtained at 60 min has the highest shear strength. In addition, based on the stress-strain curves of  $Ti_3Al/Ti_2AlNb$  joints obtained at 990 °C for 10~90 min (Fig.5b), the joint fracture is characterized by the brittle fracture.

In order to study the fracture behavior of the joint, the fracture morphology of the  $Ti_3Al/Ti_2AlNb$  joint after shear tests was observed. It is obvious that all of the fracture surfaces of  $Ti_3Al/Ti_2AlNb$  joints prepared at 990 °C for 10~90 min have typical river pattern (Fig. 6a). River pattern is the most important feature of cleavage fracture in brittle fracture, and it is formed by the confluence of several cleavage steps. According to EDS results (Table 2),  $Ti_3Al/Ti_2AlNb$  joint fracture surfaces at 10, 30 and 60 min contain a large number of Ti: Ni, and almost no Al and Nb elements appear, among which the ratio of Ti: Ni is close to 2:1. However, a significant increase in Al and Nb elements is detected on the fracture surfaces of  $Ti_3Al/Ti_2AlNb$  joint under the condition of 90 min. It shows from another aspect that too long bonding time will coarsen the grain of parent material and lead to the generation of brittle intermetallic compounds, thus affecting the strength of the  $Ti_3Al/Ti_2AlNb$  joint. Combined with XRD pattern (Fig. 3), the fracture phase of the joint is mainly  $NiTi_2$ , and there may be a small amount of NiTi and  $Al_{0.5}Nb_{0.5}Ni_3$ , indicating that the joint fracture mainly occurs in the  $NiTi_2$  layer adjacent to the  $Ti_2AlNb/Ti$  interlayer and extends to the

Table 1 EDS results of points marked in Fig.2a

Point	Composition/at%				Possible phase
	Al	Ti	Ni	Nb	
1	10.34	31.39	43.20	15.07	$Al_{0.5}Nb_{0.5}Ni_3$
2	1.41	13.19	83.31	2.09	Residual Ni layer
3	0.30	52.13	47.51	0.06	NiTi
4	1.76	66.08	31.76	0.40	$NiTi_2$
5	5.78	81.89	5.45	6.88	$Al_{0.5}Nb_{0.5}Ni_3$ +residual Ti layer
6	7.42	74.88	3.72	13.98	Residual Ti layer dissolved with Al+Nb



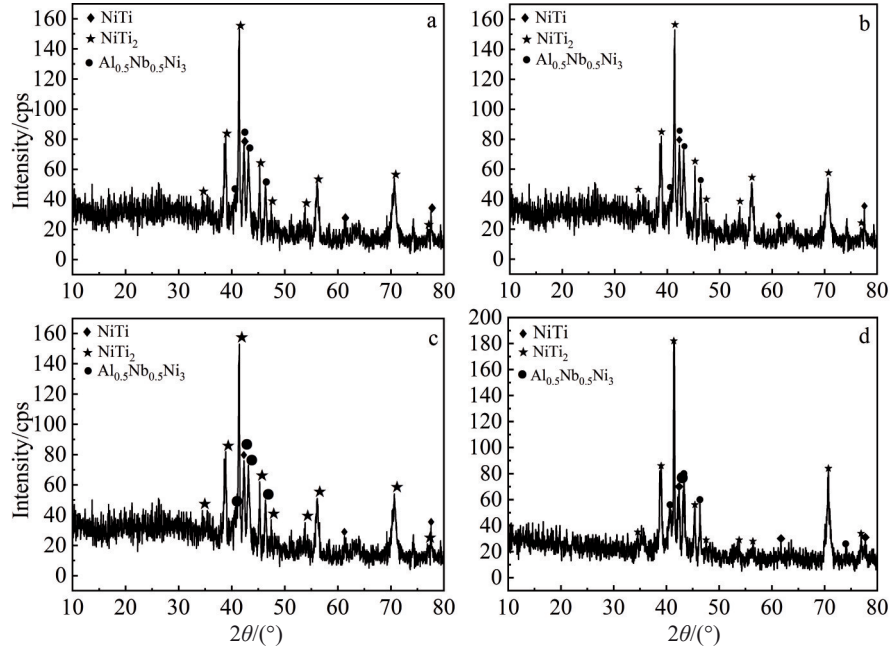


Fig.3 XRD patterns of fracture surface of  $Ti_3Al/Ti_2AlNb$  joint obtained at  $990\text{ }^\circ\text{C}$  for different bonding time: (a) 10 min, (b) 30 min, (c) 60 min, and (d) 90 min

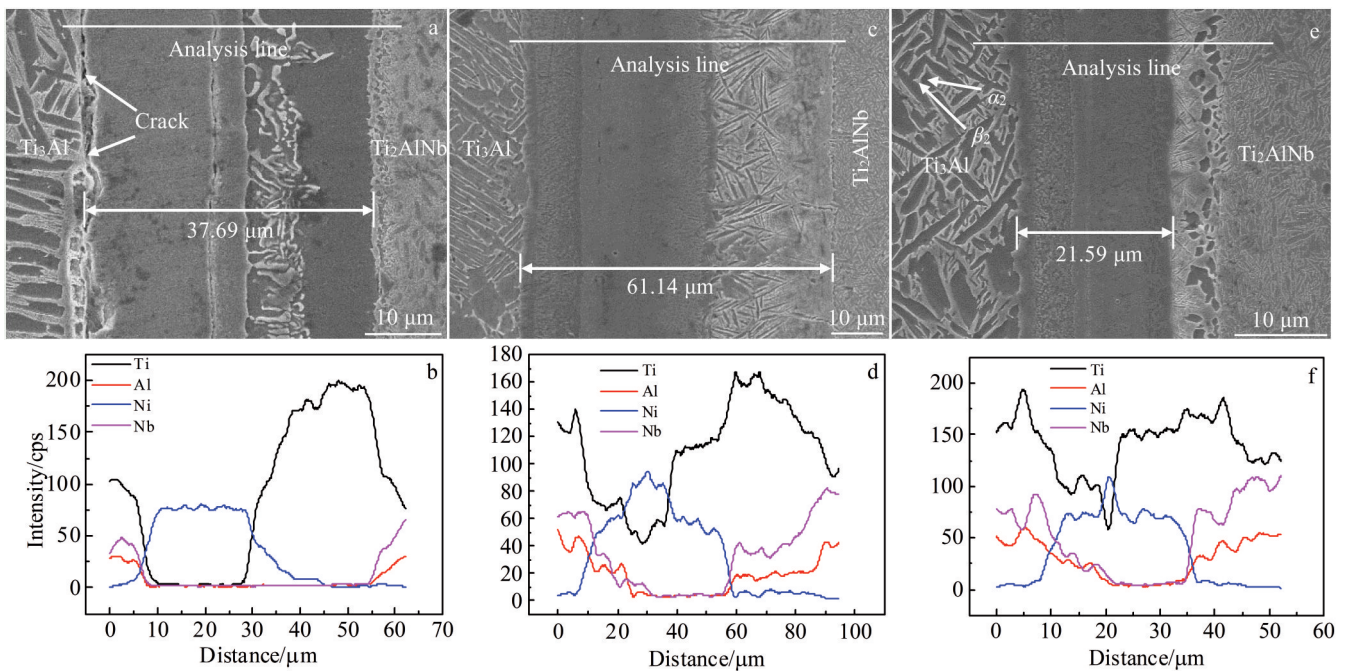


Fig.4 Microstructures (a, c, e) and EDS line scanning results along analysis line (b, d, f) of  $Ti_3Al/Ti_2AlNb$  joint obtained at  $990\text{ }^\circ\text{C}$  for different bonding time: (a, b) 10 min, (c, d) 60 min, and (e, f) 90 min

Ti interlayer.

#### 2.4 Formation mechanism of the $Ti_3Al/Ti_2AlNb$ joints

$Ti_3Al/Ti_2AlNb$  alloy joints are successfully obtained at  $990\text{ }^\circ\text{C}$  for 10–90 min. According to the analysis of interface structure and relevant references<sup>[16,20]</sup>, the formation procedure of the TLP diffusion alloy joint can be deduced. As shown in Fig.7, the bonding process of  $Ti_3Al/Ti_2AlNb$  alloy with Ni/Ti as the interlayer can be segmented into four steps. The

elaboration of each step is as follows.

(1) Surface contact stage of the joining material. The base material and the interlayer are stacked one after another, and a close physical contact forms between materials under the action of pressure.

(2) The atomic diffusion and reaction stage. When the temperature rises to eutectic reaction temperature ( $942\text{ }^\circ\text{C}$ ), Ti and Ni begin to undergo eutectic reaction, and Ti-Ni eutectic

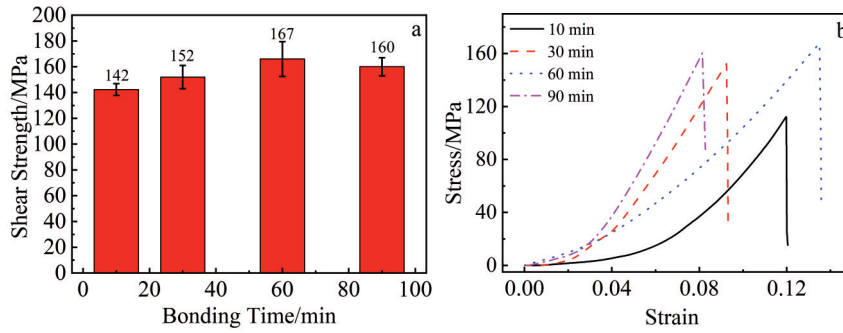


Fig.5 Shear strength (a) and stress-strain curves (b) of Ti<sub>3</sub>Al/Ti<sub>2</sub>AlNb joints obtained at 990 °C for different bonding time

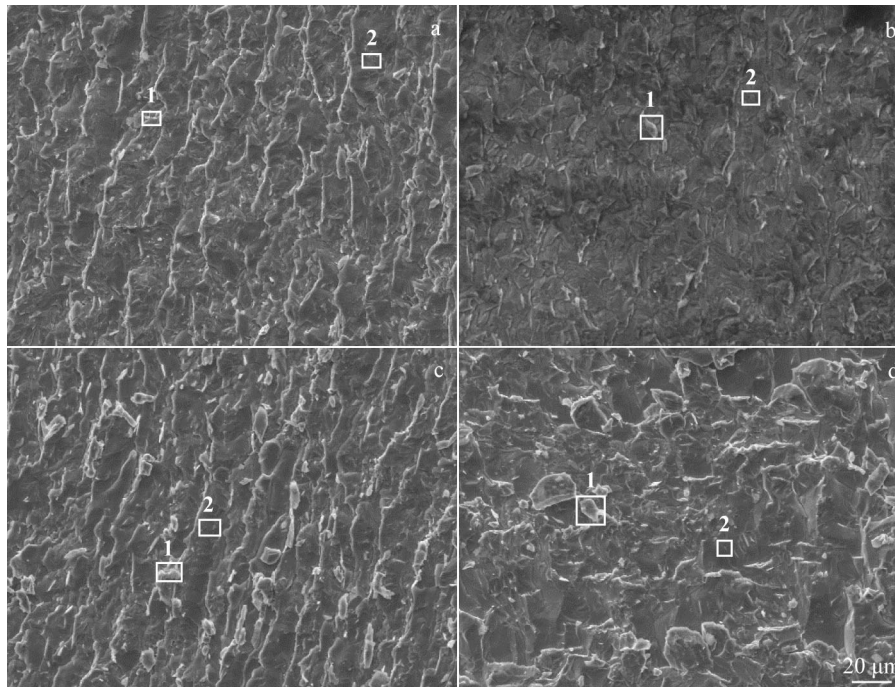


Fig.6 Surface morphologies of shear fracture of Ti<sub>3</sub>Al/Ti<sub>2</sub>AlNb joints obtained at 990 °C for different bonding time after shear tests: (a) 10 min, (b) 30 min, (c) 60 min, and (d) 90 min

Table 2 EDS result of zones marked in Fig.6

Bonding time/min	Zone	Composition/at%			
		Al	Ti	Ni	Nb
10	1	1.56	66.42	31.85	0.17
	2	1.84	69.03	28.45	0.68
30	1	5.79	61.97	30.24	2.00
	2	7.23	64.85	22.95	4.97
60	1	1.47	66.45	31.95	0.12
	2	1.48	66.39	31.95	0.18
90	1	12.10	45.61	28.21	14.08
	2	10.75	46.69	29.74	12.82

liquid phase is formed by the atom diffusion. Meanwhile, Ti and Ni foils also start to react with the base materials on both sides.

(3) Joint interface formation stage. As the temperature goes

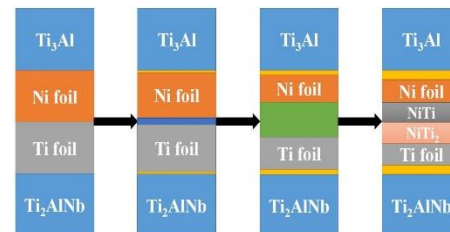


Fig.7 Schematic diagram of the forming process of Ti<sub>3</sub>Al/Ti<sub>2</sub>AlNb joint

up, the compound is generated between interlayer and parent materials. Meanwhile, Ti-Ni intermetallic compound layer will be formed between Ti and Ni foils.

(4) The complete forming stage of the joint. As the bonding time extends, the Ti-Ni eutectic phase gradually solidifies, the dense metal compound layer is formed, and the whole TLP joint composition is completely homogenized.

### 3 Conclusions

1) The  $Ti_3Al/Ti_2AlNb$  alloy joint can be prepared by TLP diffusion bonding using Ni-Ti duplex foils as interlayer under low bonding pressure. The typical interface structure of the  $Ti_3Al/Ti_2AlNb$  alloy joint can be formed as follows:  $Ti_3Al | Al_{0.5}Nb_{0.5}Ti_3 | residual Ni | NiTi | NiTi_2 | residual Ti | Al_{0.5}Nb_{0.5}Ti_3 | Ti_2AlNb$ .

2) The bonding time can significantly affect the microstructure of the  $Ti_3Al/Ti_2AlNb$  alloy joint. As the bonding time extends, the more the element diffusion, the better the chemical reaction; the overall width of the interlayer first increases and then decreases, and the thickness of residual interlayer becomes thinner, while the thickness of transition layer of adjacent parent materials increases.

3) When the bonding time reaches 60 min, the room temperature shear strength of the  $Ti_3Al/Ti_2AlNb$  alloy joint is the maximum, up to  $167 \pm 12$  MPa. In addition, the joint fracture mainly occurs in the  $NiTi_2$  layer adjacent to the residual Ti interlayer.

### References

- Naeimian H, Mofid M A. *T Nonferr Metal Soc*[J], 2020, 30(5): 1267
- Ren H S, Xiong H P, Chen B et al. *Mater Process Tech*[J], 2015, 224: 26
- Jia Qiang, Lai Zhiwei, Zhang Hongqiang et al. *Mater Process Tech*[J], 2020, 286: 116 823
- Zhu Lei, Li Jinshan, Tang Bin et al. *Vacuum*[J], 2019, 164: 140
- Li Haiyan, Zhou Yang, Cui Ao et al. *Rare Metal Materials and Engineering*[J], 2018, 47(4): 1069
- Ma Xiaodi, Xu Jiuhua, Ding Wenfeng et al. *Adv Mach Manuf Tech XII*[J], 2014, 589-590: 361
- Wang Sibing, Xu Wenchen. *Metals*[J], 2018, 8(6): 382
- Zou Guisheng, Xie Erhu, Bai Hailin et al. *Mat Sci Eng: A*[J], 2009, 499(1-2): 101
- Qu June, Guo Xingpeng, Wang Hairen et al. *T Nonferr Metal Soc*[J], 2006, 16: 2058
- Lei Zhenglong, Dong Zhijun, Chen Haibin et al. *Materials & Design*[J], 2013, 46: 151
- Cai Xiaolong, Sun Daqian, Li Hongmei et al. *Int J Precis Eng Manuf*[J], 2018,19(8): 1163
- Ren H S, Xiong H P, Long W M et al. *J Mater Sci Technol*[J], 2019, 35(9): 2070
- Ren H S, Wu X, Chen B et al. *Weld World*[J], 2017, 61(2): 375
- Azqadan Erfan, Ekrami Aliakbar. *Mater Process Tech*[J], 2017, 30: 106
- Ren H S, Xiong H P, Pang S J et al. *Metall Mater Trans A Phys Metall Mater Sci*[J], 2016, 47(4): 1668
- Wang Jie, Xiong Qinglian, Xiong Yanlin et al. *Rare Metal Materials and Engineering*[J], 2019, 48(4): 1275
- Xie Jilin, Huang Yongde, Chen Yuhua et al. *Rare Metal Materials and Engineering*[J], 2020, 49(12): 4348
- Ren H S, Ren X Y, Xiong H P et al. *Mater Charact*[J], 2019, 155: 109 813
- Lin Tiesong, Li Haixin, He Peng et al. *Intermetallics*[J], 2013, 37: 59
- Feng Yang, Wang Jie, Yang Haotian et al. *Vacuum*[J], 2020, 181: 109 752

## 保温时间对瞬时液相扩散连接的 $Ti_3Al/Ti_2AlNb$ 接头微观结构及力学性能的影响

王 杰<sup>1</sup>, 张艺伟<sup>1</sup>, 熊晏邻<sup>1</sup>, 杨 锦<sup>2</sup>, 冯 洋<sup>1</sup>

(1. 西南石油大学 新能源与材料学院, 四川 成都 610000)

(2. 成都天空燃控科技股份有限公司, 四川 成都 610500)

**摘 要:** 采用 Ni-Ti 复合箔片作为中间层, 在 990 °C、低连接压力 (0.1 MPa) 下, 通过瞬时液相 (TLP) 扩散连接制备了  $Ti_3Al/Ti_2AlNb$  异种合金接头。分析了保温时间 (10~90 min) 对  $Ti_3Al/Ti_2AlNb$  接头微观结构及力学性能的影响, 并研究了 TLP 扩散连接接头的界面演变和形成机制。结果表明,  $Ti_3Al/Ti_2AlNb$  接头具有典型的 “ $Ti_3Al | Al_{0.5}Nb_{0.5}Ti_3 | 残余 Ni | NiTi | NiTi_2 | 残余 Ti | Al_{0.5}Nb_{0.5}Ti_3 | Ti_2AlNb$ ” 多层梯度结构。随着保温时间的延长, 接头的抗剪切强度先增大后减小, 当保温时间达到 60 min 时,  $Ti_3Al/Ti_2AlNb$  接头的抗剪切强度最大, 达到  $167 \pm 12$  MPa。另外, 接头的断裂主要发生在  $Ti_2AlNb/Ti$  附近的  $NiTi_2$  层, 并向 Ti 层延伸, 呈现出脆性断裂的特征。

**关键词:**  $Ti_3Al$ ;  $Ti_2AlNb$ ; 瞬时液相; 扩散连接; 界面结构

作者简介: 王 杰, 男, 1982 年生, 博士, 副教授, 西南石油大学新能源与材料学院, 四川 成都 610000, 电话: 028-83037416, E-mail: wangjie@swpu.edu.cn